Electro-optic Measurement of the Wake Fields of a Relativistic Electron Beam

M. J. Fitch* and A. C. Melissinos
Department of Physics and Astronomy, University of Rochester, Rochester, New York 14627

P. L. Colestock,† J.-P. Carneiro,‡ H. T. Edwards, and W. H. Hartung§
Fermi National Accelerator Laboratory, Batavia, Illinois 60510
(Received 2 March 2001; published 26 June 2001)

When a relativistic electron bunch traverses a structure, strong electromagnetic fields are induced in its wake. For a 12 nC bunch of duration 4.2 ps FWHM, the peak field is measured >0.5 MV/m. Time resolution of ~5 ps is achieved using electro-optic sampling with a lithium tantalate ($LiTaO_3$) crystal and a short-pulse infrared laser synchronized to the beam. We present measurements for both the longitudinal and radial components of the field and relate them to the wall impedance.

DOI: 10.1103/PhysRevLett.87.034801 PACS numbers: 29.27.Bd, 29.25.Bx, 41.75.Ht, 52.59.–f

The development of electron accelerators with ever higher particle density is essential for applications to high energy physics, photon and x-ray sources, and free electron lasers. The electrons are produced in short pulses with low emittance that must be preserved during acceleration. Because of the impedance of the walls, and discontinuities in the beam pipe and accelerating structure, the electrons radiate, exciting wake fields in the structure. The calculation and measurement of these fields is important because they can lead to energy loss, energy spread, and emittance growth of the beam.

Electro-optic sampling of the wake fields excited by the passage of a relativistic electron beam is a noninvasive technique that offers picosecond time resolution. By suitable orientation of the electro-optic crystal it is possible to identify the different components of the electric fields and to make absolute measurements of the field strength. Applications of electro-optic sampling to high energy particle beams are discussed in Refs. [1–8].

Electro-optic sampling is based on the Pockels effect and was introduced by Auston [9] and Valdmanis *et al.* [10]. When an electric field is applied to a certain class of crystals the refractive index ellipsoid is modified, and as a result a retardation (phase shift) is introduced between two orthogonally polarized components of a pulse of light traversing the crystal. This retardation can be detected by observing the change in the polarization of the transmitted light. By using short laser pulses and varying the delay between the "probe" pulse and the pulse that produced the electron bunch, the "pump" pulse, one can sample the time dependence of the electric field.

The Fermilab high-brightness photoinjector consists of a normal conducting radiofrequency (rf) gun followed by a nine-cell superconducting cavity, for a final electron energy of 18.5 MeV. The rf frequency is 1.3 GHz. A high quantum efficiency ($\eta \sim 1\%–2\%$) Cs_2Te photocathode is installed in the rf gun. The photocathode is driven by UV laser pulses that can be shaped both in space and time. Pulse trains of typically 1 to 200 bunches (up to 12 nC charge per bunch) spaced 1 μs apart can be accelerated at a repetition rate of 1 Hz. The measured normalized emittance of the beam was measured to be $\epsilon \simeq 2$ (20) mm mrad at a charge 1 (12) nC. The bunch length after compression varied from $\sigma = 2.3$ to 4 ps depending on the beam charge, 1–8 nC. Details of the gun and beam line design can be found in Refs. [11–13].

The arrangement used in our experiment is shown schematically in Fig. 1. The laser produces a 1 MHz train of pulses in the IR ($\lambda = 1054$ nm) [14]. These pulses of energy ~100 μJ are compressed in a set of gratings to a width of 2–3 ps and then quadrupled to the UV. The UV pulse is now lengthened in a pulse stacker [15,16] to a flattop of 10 ps FWHM and sent to the cathode. Part

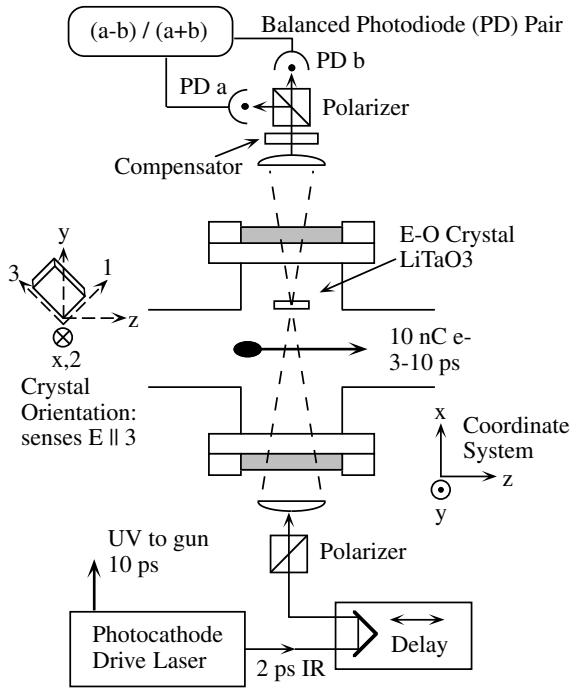

FIG. 1. Schematic layout of the electro-optic sampling arrangement. Note the coordinate system used and the orientation of the $LiTaO_3$ crystal.

of the unconverted IR is used as the probe pulse and is routed to the electro-optic crystal via a variable optical delay stage. The stage can be moved with subpicosecond resolution, and, with a hollow corner cube retroreflector, maintains pointing stability over its entire range of 3 ns.

The electro-optic crystal is placed in the vacuum in a diagnostic cross in the electron beam pipe; the laser probe pulse propagates normally to the electron beam direction passing through entrance and exit windows. The coordinate convention used is indicated in Fig. 1. The electron beam propagates along z, the probe laser pulse along x, y is the up-going vertical, and x-y-z form a right-handed system.

The crystal is a 1.5 mm thick piece of $LiTaO_3$ of dimensions 7 mm $\times$ 8 mm. To measure the tangential field, the crystal is placed at a distance of 2 cm from the center of the beam pipe with its extraordinary axis (3-axis) in the y-z plane, and rotated 45° relative to the horizontal. The thin dimension of the crystal, its 2-axis, coincides with the x axis (horizontal); the laser probe beam propagates along the x axis with linear polarization along the y axis. The two polarizations of the transmitted beam are analyzed by a cube beam splitter and recorded by two separate fast photodiodes. A $\lambda/4$ plate allows us to balance the two diodes in the absence of a field. We record the intensity I_a, I_b incident on each diode and form the asymmetry R

$$R \equiv \frac{I_a - I_b}{I_a + I_b} = \sin\Gamma \approx \Gamma\,, \tag{1}$$

where Γ (in radians) is the phase retardation

$$\Gamma = 2\pi(\ell/\lambda)\,\frac{1}{2}\,(n_e^3 r_{33} - n_o^3 r_{31})E_z/\sqrt{2}\,. \tag{2}$$

Here $\ell = 1.5$ mm is the length of the crystal, λ the wavelength, n_e and n_o the extraordinary and ordinary refractive indices, and r_{33} and r_{31} the corresponding components of the electro-optic tensor [17]; E_z is the electric field. (The same coefficient applies to E_y, since the crystal's 3-axis lies 45° between y and z. The electro-optic coefficient for other directions is ~20 times smaller.) From the published values for $LiTaO_3$ we expect for our configuration $\Gamma = 0.099E_z/(100\ \mathrm{kV/m})$. From an experimental calibration of the crystal we found $\Gamma = 0.046E_z/(100\ \mathrm{kV/m})$, and we used this value to estimate the electric field.

For each position of the delay stage, typically we averaged four pulses with the electron beam and recorded one background pulse (no electron beam). This permitted us to carry out a background subtraction and thus eliminate a drift of the baseline arising from slow changes in the static birefringence of the crystal. The typical step size was 1 ps and the sampling was carried out to 3 ns.

Results obtained for the longitudinal component are shown in Fig. 2a in the time domain. The background data have been smoothed and subtracted from the signal data. Figure 2b gives the same data in the frequency domain. The resolution of the frequency spectrum is determined by the length of the record $\Delta f = 1/\Delta T$ (typically 0.2 GHz)

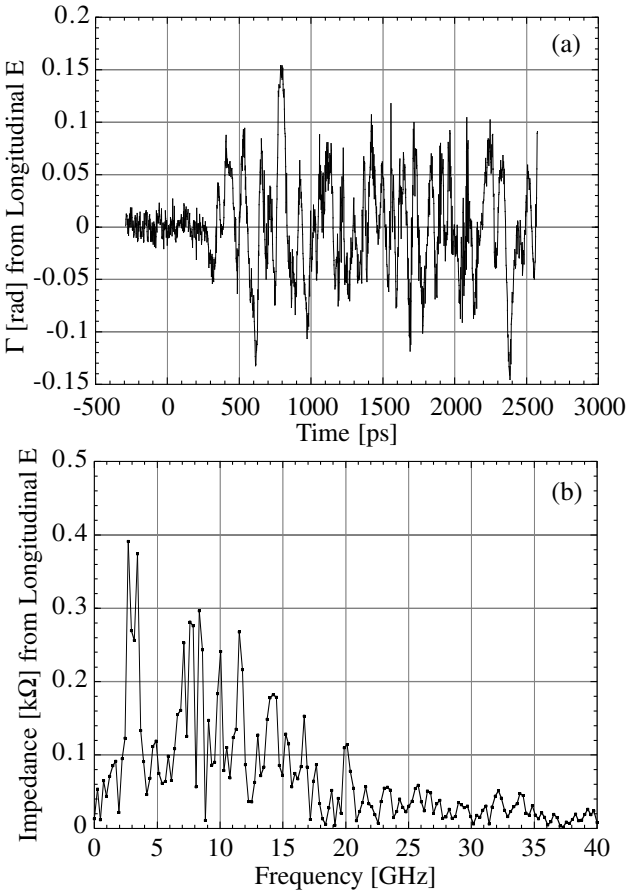

FIG. 2. (a) Measured tangential electric field as a function of time after the arrival of the electron bunch. The ordinate represents the measured polarization asymmetry $R \simeq \sin\Gamma$. (b) Fast Fourier transform of the time domain data, which is a direct measure of the wall impedance. The ordinate is calibrated in ohms.

and the extent of the spectrum by the time step size, τ; $f_{\max} = 1/2\tau$. The crystal in the configuration shown in Fig. 1 is sensitive to E_z and E_y with the beam proceeding along z. Thus the crystal is sensitive to TE-like modes excited in the cross pipes which are normal to the beam direction. Comparing the predicted frequencies for a cylindrical cavity with the same dimensions of the cross arms to the observed frequencies (from the data shown in Fig. 2) gives reasonable agreement for some peaks. The predicted (observed) frequencies in GHz are 7.68 (7.7) TE_{010}, 8.43 (8.3) TE_{310}, 10.69 (10.1) TE_{120}, 14.07 (14.0) TE_{020}, 16.07 (16.4) TE_{320}, and 20.39 (19.8) TE_{030}. The lowest two peaks at 2.7 and 3.4 GHz roughly agree with MAFIA results for an ideal six-way cross. From Tang and Ng's calculations [18] scaled from a 35 mm cross to our 48 mm cross, there is a TE_{111}-like mode at 2.9 GHz and a TE_{211}-like mode at 3.5 GHz. Of course, the measurement is not made in an ideal (empty) six-way cross, but one with a crystal and mount, glass view ports, and a beam flag.

To probe the radial mode of the electric field (in this case E_x), the crystal was rotated so that its plane surface was normal to the beam, and the 3-axis is now radial (in this

case along x). The laser probe beam was bent using a pair of prisms to propagate along the crystal 2-axis (aligned now parallel to z). The results in the time domain are shown in Fig. 3a and in the frequency domain in Fig. 3b. The resonant structure is quite different and corresponds to the TM modes of a cylindrical cavity. The dominant mode at 8.8 GHz can be roughly identified with the TM_{110} mode predicted at 7.7 GHz. These data were obtained with a bunch charge of 8 nC and bunch length $\sigma = 3.5$ ps.

The work done by the wake field is expressed by the wake potentials [19,20]. For a localized (point) bunch the wake potential is the integral of the fields at a distance s behind the bunch. The integration extends over the active structure and the wake potential is normalized to unit charge.

$$\vec{W}_\delta(r_1, s) = \frac{1}{q} \int_{-\infty}^{+\infty} dz [\vec{E}(r_1, z, t) + \vec{v} \times \vec{B}(r_1, z, t)]_{t=(z+s)/c} . \tag{3}$$

For a beam centered on axis, r_1 is the transverse distance and q the bunch charge. Generalizing from a point bunch to a charge distribution $\lambda(s)$ [normalized to unity $\int_{-\infty}^{\infty} \lambda(s')\, ds' = 1$], the wake potential is the convolution:

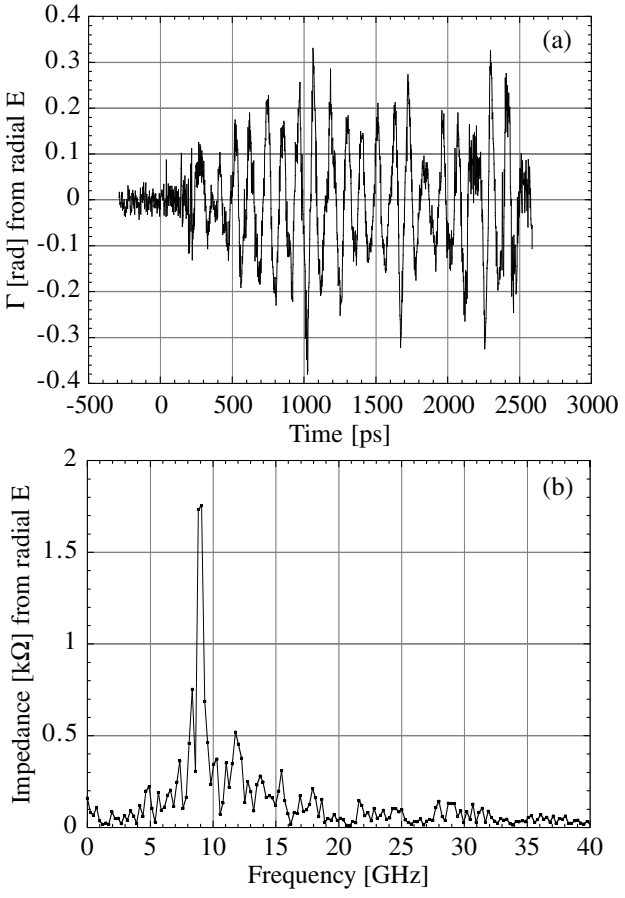

FIG. 3. As in Figs. 2a and 2b but for the radial component of the electric field.

$$\vec{W}(\vec{r}_1, s) = \int_0^{\infty} ds'\, \lambda(s - s') \vec{W}_\delta(\vec{r}_1, s) . \tag{4}$$

Finally, the potentials are separated into a longitudinal and transverse part. For the longitudinal potential the dependence on r_1 is dominated by the monopole term, whereas for the transverse potential, the dipole term is dominant.

Since the fields are appreciable only over the aperture of the six-way cross, the integration in Eq. (3) can be approximated by

$$W(r, s) \simeq \frac{1}{q} E(r, t)_{t=s/c} \Delta z , \tag{5}$$

where Δz is of the order of the beam pipe diameter. To account for the time dependence of the wake fields, which is omitted from Eq. (5) we have averaged over the beam pipe aperture and use for Δz only one-half of the diameter. The longitudinal and transverse impedances, $Z_\parallel$ and $Z_\perp$ are given by the real part of the Fourier transform of the wake potentials, i.e.,

$$Z_\parallel(r, \omega) \tilde{\lambda}^*(\omega) = \frac{1}{c} \int_{-\infty}^{+\infty} W_\parallel(r, s) e^{-i(\omega/c)s}\, ds . \tag{6}$$

The longitudinal impedance is shown in Fig. 2b where the ordinate has been labeled accordingly, using the measured electro-optic calibration as above and dividing by the mean charge for the scan. The wake fields were measured off-axis, the crystal being located at a distance of 3 cm from the beam. Since the longitudinal wake potential is dominated by the monopole term, we assume that the wake field is independent of the transverse position. However, the measured longitudinal field at the location of the crystal can contain components that do not contribute to the longitudinal wake. Our measurements do not allow us to differentiate between these different contributions.

A similar analysis can be carried out for the transverse impedance. However, in this case the magnetic field which contributes to the impedance is not measured. Furthermore, the dependence of the transverse component of the field on the distance from the beam axis at which the field was measured is not known.

With these reservations we show in Fig. 3b the Fourier transform of the transverse electric field and have converted the ordinate to units of impedance as before. These data were obtained for a bunch length of 6 ps FWHM ($\sigma_z = 0.77$ mm) and give a qualitative measure of the transverse beam impedance.

A calculation of the wake fields excited in a six-way cross has been recently carried out [21] using MAFIA and the results are in reasonable agreement with the data. Most analytic calculations, however, return the loss factors $k_\parallel$ and $k_\perp$ which can be obtained in the frequency domain by

$$k_\parallel = \int_{-\infty}^{+\infty} |\tilde{\lambda}(\omega)|^2 Z_\parallel(\omega)\, d\omega , \tag{7}$$

where $\tilde{\lambda}(\omega)$ is the Fourier transform of the electron beam longitudinal charge distribution $[\int \lambda(z)\, dz = 1]$. Since the bunch length is much shorter than the wavelength of the frequencies of interest, the factor $|\tilde{\lambda}(\omega)|^2$ is only a 0.95 correction at 20 GHz. For a 48 mm six-way cross,

Tang and Ng [18] used MAFIA to find $k_{\parallel} = 1.73$ V/pC for a bunch of length $\sigma_z = 0.8$ mm. In the approximation of Eq. (5), we weight the data of Fig. 2b with $\lambda(\omega)$ and integrate over frequency to obtain a measured value of $k_{\parallel} = 1.9 \pm 0.2$ V/pC in excellent agreement with the calculation.

For the transverse loss factor $k_{\perp}$ it is conventional to report the dipole term $k_{\perp} = (1/r) \int |\tilde{\lambda}(\omega)|^2 Z_{\perp}(\omega)\, d\omega$, where r is the distance from the beam axis. We have integrated the data of Fig. 3b and set $r = 3$ cm, the distance from the beam axis to the crystal, to obtain $k_{\perp} = 50 \pm 6$ V/pC $\cdot$ m for $\sigma_z = 0.9 \pm 0.1$ mm. The corresponding calculated value [18] is 12 V/pC $\cdot$ m. However, for $\sigma_z = 3.4 \pm 0.3$ mm we find from the data $k_{\perp} = 30 \pm 6$ which agrees with the calculated value of $k_{\perp} = 24$ V/pC $\cdot$ m. In the calculations the effects of the crystal and of other insertions in the vertical arms of the cross were not included. More importantly, neglecting the contribution of the magnetic field to $k_{\perp}$, as well as the assumptions made in extracting $k_{\perp}$ from the data preclude an exact comparison with the calculated values.

When this study originated we expected that the direct field of the bunch would dominate in the time domain, and would give a measurement of the electron bunch length. This was not observed even though the time resolution of our measurement was comparable to the bunch length. The absence of the direct field is not understood at this time. So far, modeling [21] has not shown any interferences from the bending prisms used in the radial E geometry. Observation of the direct field of a freely propagating beam has been reported by Yan *et al.* [8].

In conclusion, we have demonstrated that electro-optic sampling can be used to measure directly and with ps resolution the wake fields excited by relativistic electron bunches in an arbitrary structure and to determine the impedance of the structure. The agreement with calculated values is at the expected level given the difficulties in modeling a realistic structure and the experimental uncertainty. Conventional rf techniques, such as in Ref. [22], have a frequency reach of a few GHz, while electro-optic sampling has been shown [23,24] to recover frequencies of tens of THz. This corresponds to a time resolution well below 100 fs, which is well beyond the resolution of streak cameras. Furthermore, by using a chirped optical pulse [25] single shot measurements have been demonstrated.

We thank our colleagues on the AØ Photoinjector and the Fermilab Beams Division for continued support. Fermilab is operated by the Universities Research Association for the U.S. Department of Energy under Contract No. DE-AC02-76CH03000. This work was carried out in part under DOE Grant No. DE-FG02-91ER40686.

*Present address: Institute of Optics, University of Rochester, Rochester, NY 14627.

†Present address: Los Alamos National Laboratory, Los Alamos, NM 87545.

‡Present address: Université Paris Sud F-91405 Orsay, France.

§Present address: NSCL/Cyclotron Lab Michigan State University, East Lansing, Michigan 48824.

[1] P. J. Channell, Los Alamos National Laboratory, Technical report, Accelerator Theory Note AT-6:ATN-82-1, 1982 (unpublished).

[2] Yu. S. Pavlov and N. G. Soloviev, in *Proceedings of the 8th All-Union Conference on Charged Particle Accelerators, Protvino, USSR, 1982*, edited by A. A. Vasilev (Joint Institute for Nuclear Research, Protvino, USSR, 1982), Vol. 2, pp. 63–67.

[3] TESLA Collaboration, M. Geitz, K. Hanke, and A. C. Melissinos, DESY Technical report, 1997 (unpublished).

[4] Y. K. Semertzidis *et al.,* in *Proceedings of the 1999 Particle Accelerator Conference,* edited by A. Luccio and W. MacKay (IEEE, New York, NY, 1999), pp. 490–491.

[5] M. J. Fitch *et al.,* in *Proceedings of the 1999 Particle Accelerator Conference* (Ref. [4]), pp. 2181–2183.

[6] G. M. H. Knippels *et al.,* Phys. Rev. Lett. **83**, 1578 (1999).

[7] D. Oepts *et al.,* in *Proceedings of the 1999 Free-Electron Laser Conference,* edited by J. Feldhaus and H. Weise (Elsevier Science, Amsterdam, 1999), Pt. II, p. 57.

[8] X. Yan *et al.,* Phys. Rev. Lett. **85**, 3404 (2000).

[9] D. H. Auston, Appl. Phys. Lett. **26**, 101 (1975).

[10] J. A. Valdmanis, G. Mourou, and C. W. Gabel, Appl. Phys. Lett. **41**, 211 (1982).

[11] E. R. Colby, Ph.D. thesis, University of California at Los Angeles, 1997.

[12] E. R. Colby, in *Proceedings of the 19th International Linear Accelerator Conference,* edited by C. E. Eyberger, R. Pardo, and M. White (Argonne National Laboratory, Chicago, 1998), pp. 758–762.

[13] J. P. Carneiro *et al.,* in *Proceedings of the 1999 Particle Accelerator Conference* (Ref. [4]), pp. 2027–2029.

[14] A. R. Fry, M. J. Fitch, A. C. Melissinos, and B. D. Taylor, Nucl. Instrum. Methods Phys. Res., Sect. A **430**, 180 (1999).

[15] M. J. Fitch, Ph.D. thesis, University of Rochester, 2000.

[16] C. W. Siders *et al.,* Appl. Opt. **37**, 5302 (1998).

[17] See, for instance, A. Yariv, *Optical Electronics* (Holt, Rinehart and Winston, New York, 1985), Chap. 9.

[18] Ch. X. Tang and J. Ng, DESY TESLA Technical Report No. 97–11, 1997 (unpublished).

[19] A. W. Chao, *Physics of Collective Beam Instabilities in High Energy Accelerators* (John Wiley and Sons, New York, 1993).

[20] P. B. Wilson, in *Physics of Particle Accelerators: Proceedings of the Fermilab Summer School, 1987 and the Cornell University Summer School, 1988,* edited by M. Month and M. Dienes, AIP Conf. Proc. No. 184 (AIP, New York, 1989).

[21] S. Wipf (private communication).

[22] A. Palmieri *et al.,* Phys. Rev. ST Accel. Beams **3**, 112001 (2000).

[23] Q. Wu and X.-C. Zhang, Appl. Phys. Lett. **71**, 1285 (1997).

[24] A. Leitenstorfer *et al.,* Appl. Phys. Lett. **74**, 1516 (1999).

[25] Z. Jiang and X.-C. Zhang, IEEE J. Quantum Electron. **36**, 1214 (2000).